Image analysis of plastic deformation in the fracture of paper

DERRICK M. S. WANIGARATNE†, WARREN J. BATCHELOR*, ANDREW B. CONN§ AND IAN H. PARKER#

A new imaging technique has been developed to characterise the outer plastic deformation field resulting from a fracture process in a sample of deep Double–Edge Notched Tension (DENT) geometry. This technique has the ability to measure strains of less than 0.1%. Commercial copy paper samples were used during the establishment of this technique. The results indicate that the plastic deformation field for fracture in the CD direction is more significant than that for fracture in the MD direction.

Keywords
Fracture toughness, DENT geometry, fracture process zone (FPZ), image analysis

The fracture toughness (FT) of a material is its ability to resist the propagation of existing cracks or flaws when under stress. For paper, FT is a fundamental mechanical parameter, which is important in manufacturing and printing or other transformation operations. This is because paper web breaks resulting from insufficient FT cause significant financial losses to the industry. Paper runnability studies have shown that most web breaks originate from intrinsic defects such as shives, holes etc. in the paper web (*1*).

In paper manufacturing and other converting operations most of the loads are applied in the plane of the sheet. Although the industry traditionally uses Elmendorf or similar tear tests to evaluate the resistance of paper to crack propagation, these types of tests have been criticised because they involve out-of-plane forces. In-plane FT testing techniques have been considered as alternatives to the Elemendorf tear test (*2,3*). Direct application of Linear Elastic Fracture Toughness Mechanics (LEFM), which is appropriate for ideal elastic materials, was tested for applicability to paper as long ago as 1975 (*4*).

†Student, *Lecturer, §Research Fellow, #Associate Professor
Australian Pulp and Paper Institute
Department of Chemical Engineering
Monash University, P.O. Box 36 Clayton, Australia

When sufficiently large tensile stresses are applied to a paper sheet containing a crack, rupture of fibre-fibre bonds and fibres occurs in a region ahead of the advancing crack tip. This region is commonly called the Fracture Process Zone (FPZ). For an elastic material the FPZ is small and all permanent deformations are confined to this region. The irreversible work associated with the fracture process in the FPZ is defined as the specific essential work of fracture of the material (*5*). The FT of a material is the specific essential work of fracture per unit crack area. While the specific essential work of fracture is easy to measure for an elastic material, only paper made from mechanical pulps is linear–elastic to fracture. Paper made from chemical pulps generally displays elastic–plastic behaviour and has a low yield stress.

When an elastic–plastic material is strained, irreversible deformations occur not only in the FPZ but well outside this region. Application of LEFM is not simple for an elastic-plastic material like paper since plastic deformation occurs outside the FPZ. The work consumed in a region outside the FPZ is not essential to the fracture. The area under a non-linear load–extension curve obtained by applying tensile loads to a cracked specimen represents both essential and non-essential work. Thus to successfully measure the fracture toughness of an elastic-plastic material the essential and non-essential work must be separated.

In the measurement of the FT of ductile materials, two non-linear elastic methods: the '*J*-integral' (*6*) and 'essential work of fracture' (*7*) approaches have been used. In the *J*-integral method, the specific fracture energy or the critical value of the strain energy release rate has been described as a line integral around the crack tip. The *J*-integral method has been applied to paper for measuring specific fracture energy (*8,9*).

The other method, the essential work of fracture technique (EWF), has the ability to separate essential and non-essential work involved in the process of fracture. This method uses the deep Double–Edge Notched Tension (DENT) geometry, which consists of notches, where fracture is initiated, cut either side of a central ligament of length (L), as shown in Figure 1. It has been tested for various

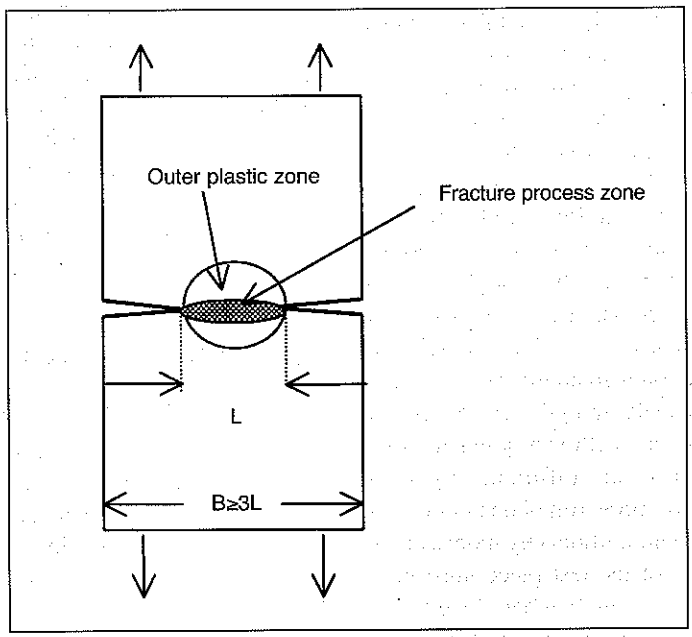

Fig. 1 A sample of deep Double–Edge Notched Tension (DENT) geometry. (B = specimen width, L = ligament length)

handsheets and commercial papers (*10*). If the shape of the outer plastic zone is assumed to be circular then the non-essential work of fracture will be proportional to L^2, while the essential work of fracture will be proportional to L.

Assuming the outer plastic zone is circular, the total work of fracture W_f is expressed mathematically (*10*) as,

$$W_f = w_e Lt + \beta L^2 t w_p \quad [1]$$

Which can be rewritten as,

$$w_f (=W_f/Lt) = w_e + \beta L w_p \quad [2]$$

where

W_f = total work of fracture
w_e = work consumed per unit crack area (FT)
L = ligament length
t = thickness of the sample
β = shape factor for the outer plastic zone
w_p = non-essential work dissipated per unit volume of the material

The fracture toughness, w_e can then be obtained from the y-intercept of a plot of w_f against L.

With either the *J*-integral or essential work of fracture techniques, the fracture toughness should be an intrinsic property of the material and independent of specimen or crack geometry. However, it has been shown that in some situations the values obtained using the *J*-integral method are not completely independent of sample or crack geometry (*3*). In addition, when values of fracture toughness measured by the two techniques are compared, it is found that the *J*-integral method seems to determine the fracture toughness correctly only for brittle, low fracture toughness papers. For ductile, high fracture toughness papers, it seems to seriously underestimate the fracture toughness (*11*).

The main advantage of the *J*-integral method is that it is relatively simple and can be done on a standard size strip used for testing tensile strength. As the essential work of fracture method requires multiple measurements at different ligament lengths, it is more time-consuming and consumes disproportionately more sample, as the width of the test piece must be at least three times the ligament length. The time and effort required for a FT measurement could be reduced if the work in the outer plastic zone could be estimated without needing measurements at multiple ligament lengths. In order to achieve this, more information about the work in the outer plastic zone is required.

So far only a few attempts have been made to observe or estimate the size of the surrounding outer plastic zone during fracture and also to test the validity of equation [2] for paper. Infra-red thermography has been used to visualise the plastically deformed region as a function of temperature (*12*). The deformed area was observed to be circular but no quantitative measurements of permanent strain in this region were obtained. Further thermographic studies carried out by Tanaka and Yamauchi (*13*) on DENT specimens have classified the developing pattern in the plastic deformation zone into three categories. A deformation field that extends through the whole ligament and eventually develops into a circular or oval zone before or at the maximum load point was designated as type I. Specimens with small ligament lengths (L<6 mm) were found to belong to this category. A deformation field that begins from both notch tips and then extends and overlaps to form a circular or oval zone after the maximum load point is reached was designated as type II. A deformation field that appears from both notch tips and does not extent to form a single plastic deformation field before final failure was categorised as type III. Specimens with larger ligament lengths were identified as belonging to type II or III.

Electronic speckle photography has also been used to determine the local displacements in the region of the crack tip. A study using this technique was carried out to estimate the critical load prior to crack propagation, which is required in the *J*-integral approach (*14*).

The present paper discusses a novel image analysis technique that has been developed to estimate the plastic strain in the deformation field.

EXPERIMENTAL METHOD

Sample preparation

Samples with DENT geometry and ligament length L ≤ 1/3B (B=sample width) were tested. Graphic design software was used to print very fine vertical lines, 250 μm apart, on the sample. Additional larger horizontal lines, drawn 2 mm apart, were used as guide lines to locate regions of interest in the sample during testing. This design was printed on the paper sample using a HP LaserJet 5MP, 600 dpi laser printer. The paper was fed into the printer to obtain fine lines normal to the straining direction.

For the initial tests presented here, samples of 80 g/m^2 (~ 100 μm thickness) 'REFLEX' commercial copy paper with dimensions of 100 mm (span) x 60 mm (width) and L=15 mm (L/B = 0.25) were used. The double notches were introduced to the sample using a specially designed 'cutting-jig' consisting of two sharp tool blades, one of which is adjustable to obtain the required ligament length. The jig was mounted in a Fly-press (consisting of quick action multiple start threads in a spiral track), which enabled a uniform force to be applied to improve the reproducibility of cutting of the fine notches. Samples were then conditioned at 23°C and 50% RH and all the tests were carried out at the same conditions. In the work that follows, samples are identified as either MD or CD. These labels indicate that the samples were cut so that the tensile load was applied along the indicated directions.

Image analysis

Images of the region of interest (ROI) were captured using an OLYMPUS SZ40 microscope, a PULNiX TM–6CN CCD camera and a personal computer equipped with a MACH Series DT 3155 frame capture card (see Fig. 2), before and after in–plane straining.

As equation [2] was derived assuming that the outer plastic zone is circular with a diameter L, the images for this analysis covered an area larger than this circular zone. To accomplish this task a series of images, at a spacing of 1.25 mm, was captured along a 25 mm line, normal to and centred on the ligament. The microscope magnification was set to capture images containing 7 or 8 lines (in an area of about 2x2 mm^2) so that the average line spacing could be obtained accurately.

Figure 3 illustrates a ROI of a sample near the crack tip. A typical captured image is shown in Figure 4. Optimas image-processing software was used to obtain an average gray scale value for each pixel in a line parallel to the direction of the applied stress. The gray scale values were inverted by subtracting them from the maximum gray scale value of 255 to obtain the lines as peaks rather than valleys. The resulting data were exported as a text file. The centres of the peaks and Full

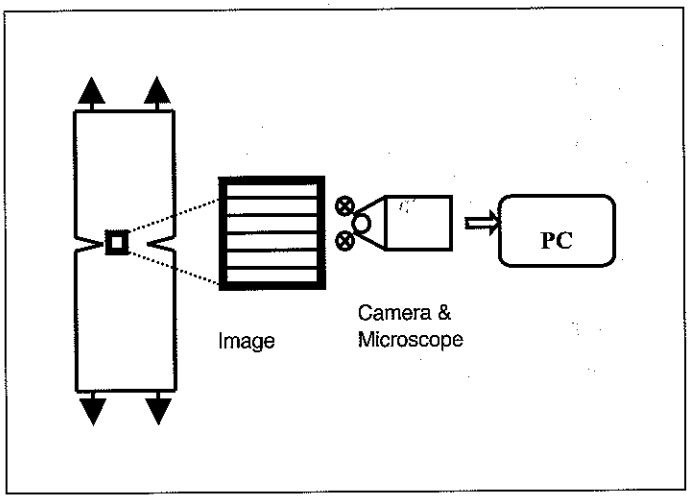

Fig. 2 Experimental set up for image capturing system.

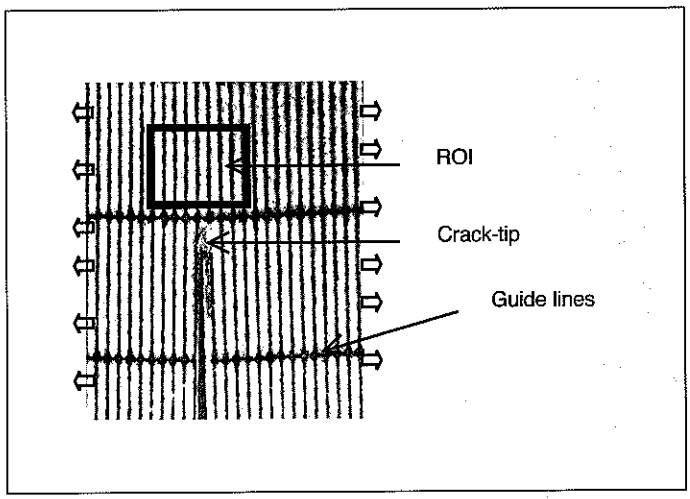

Fig. 3 Part of a DENT sample near a crack tip.

Width Half Maximum (FWHM) were obtained using a peak–fitting program. Figure 5 shows a typical inverted gray scale plot (for the image in Figure 4) with the fitted curve obtained from the peak-fitting program. Finally, with aid of spreadsheet software, the average line spacing and the uncertainties for each image were obtained.

Sample straining

The samples were strained using a specially designed (*15*) pair of line type clamps mounted on an Instron, model 5566 universal testing machine. The crosshead speed of the Instron was set at 0.5 mm/minute. Two guide rods with low friction, high-precision linear bearings, ensured that the sample was loaded in–plane. A microscope was used to observe the notch tip and to determine the critical point to stop straining before the crack began to propagate.

Calibration

To check the accuracy of the technique for determining strain, real-time images of the middle of a printed CD tensile test piece (dimensions 100 mm x 13 mm) of commercial copy paper were captured using the image capturing system while straining at the above rate. The printed lines were normal to the applied stress. The frames were captured at a rate of 1.8 frames/second. A comparison was obtained between the set linear strain rate (0.0083% per sec.) and the experimental strain rate determined by image analysis.

Real-time images of an area close to the crack-tip (an area similar to that shown in Fig. 3 as ROI) of a DENT sample were also captured. The cross-head speed was set to 2 mm/minute in this test. The line spacing variation or strain of this region with respect to the linear crosshead speed of the Instron was obtained.

CALIBRATION RESULTS

CD Tensile test piece

Figure 6 shows the results obtained from the CD tensile test piece. The strain rate of the tensile sample was measured to be 0.0091% ± 0.0003% per second, at a set strain rate of 0.0083% per second. There is thus a small difference between the experimental and set strain rates. However, considering the fact that the paper is non-uniform (i.e. local and global strain rates differ), these results can be considered as quite reasonable. The most significant feature is the resolution of the technique, which was better than 0.01 pixel (0.03 μm). Therefore this technique has the ability to measure strains of less than 0.1% in this particular measurement system.

DENT Specimen

Non-linear line spacing variation is clearly evident in the DENT (CD) sample

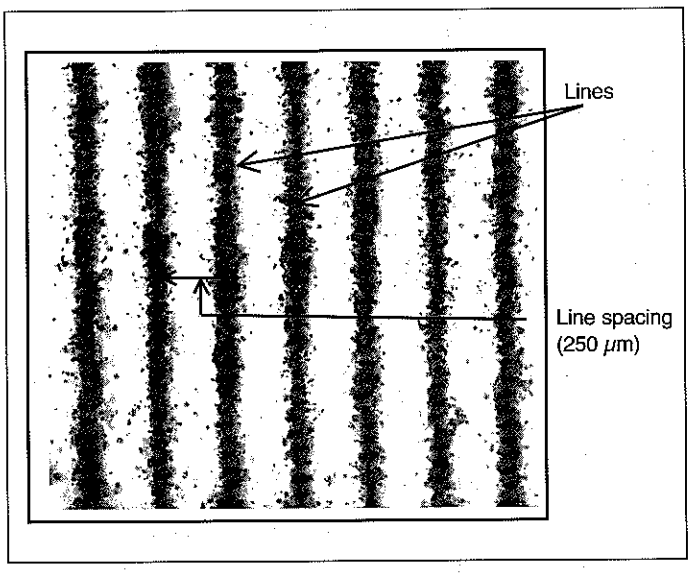

Fig. 4 A typical image showing 7 lines. (Lines are 250 μm apart).

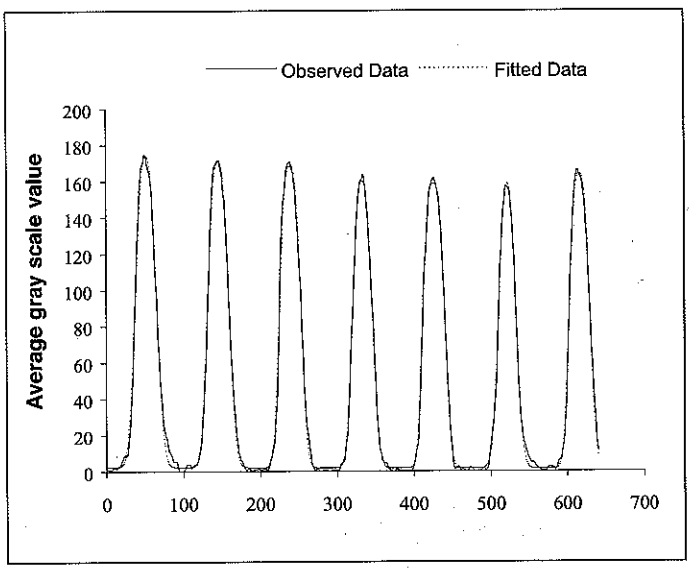

Fig. 5 Inverted average gray scale plot for image in Figure 4. Broken line gives the fitted curve.

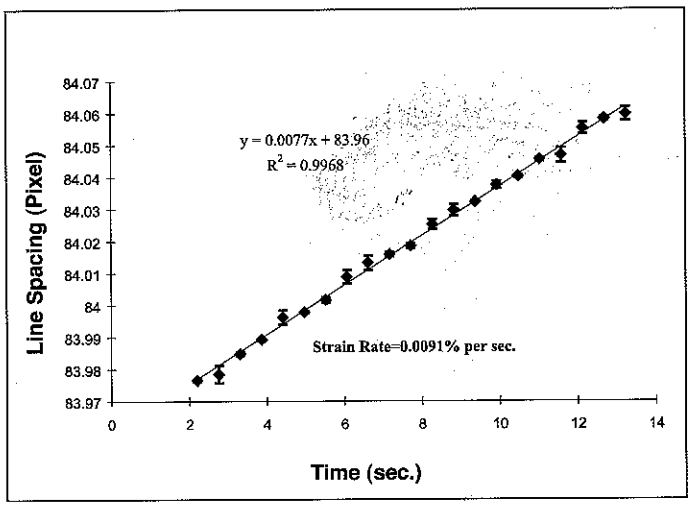

Fig. 6 Line-spacing variation of a CD tensile test piece of copy paper with time.

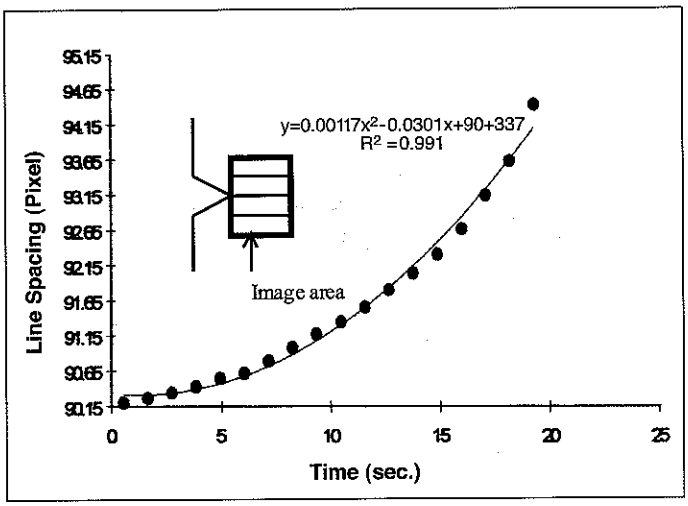

Fig. 7 Line spacing variation of DENT sample near the crack tip. Left insert shows an expanded view of the image area.

subjected to constant elongation (see Fig. 7). This behaviour is a result of high stress concentration at the crack-tip compared to the stress distribution in other areas of the sample.

RESULTS AND DISCUSSION

The CD and MD load–elongation behaviour of DENT samples is shown in Figure 8. A linear variation in the first part of the curve (up to about 0.2 mm extension) in the CD direction indicates an elastic type straining. The deviation from linearity in the latter part of the curve is indicative of elastic-plastic behaviour. For the loading in the CD direction the maximum load and extension obtained just before crack propagation were about 33 N and 0.5 mm respectively.

Figure 9 shows the variation in the average line spacing, in pixels, for each image captured along the first guide-line in the CD. The x-axis gives the distance from the ligament to the centre point of the image.

One data set (filled circles) shown in this figure was obtained from images captured before straining the sample. A second set (open circles) was obtained from images captured soon after the straining. A third set (filled diamonds) was obtained from the images captured after leaving the sample at 23°C and 50% RH for nearly 16 hours. It is assumed that this is an adequate time for any strain recovery to have occurred. In the second data set, the image located close to the middle of the ligament (0 mm distance) has the highest line spacing. The estimated average line spacing for this image was 92.04 pixels. The average line spacing for the corresponding image in the third set was 91.92 pixels. The reduction in line spacing of 0.12 pixels corresponds to an absolute 0.13% reduction in strain.

The maximum change in line spacing due to straining of the sample (for the image at the ligament) was about 1.4 pixels. This is equal to an absolute plastic strain of 1.48%.

Figure 10 shows the strain (%) as a function of position along 5 guide-lines normal to the ligament length. The position of maximum strain (%) along each guide-line was at the ligament position except for that obtained along the 4th guide-line. The position of maximum strain along the

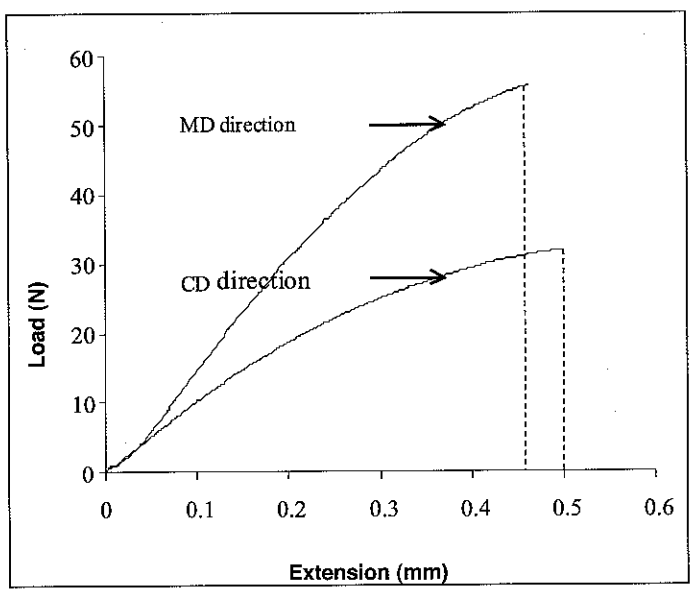

Fig. 8 Load against extension data for copy paper in the CD and MD directions on a DENT sample. In both instances straining was stopped before crack propogation.

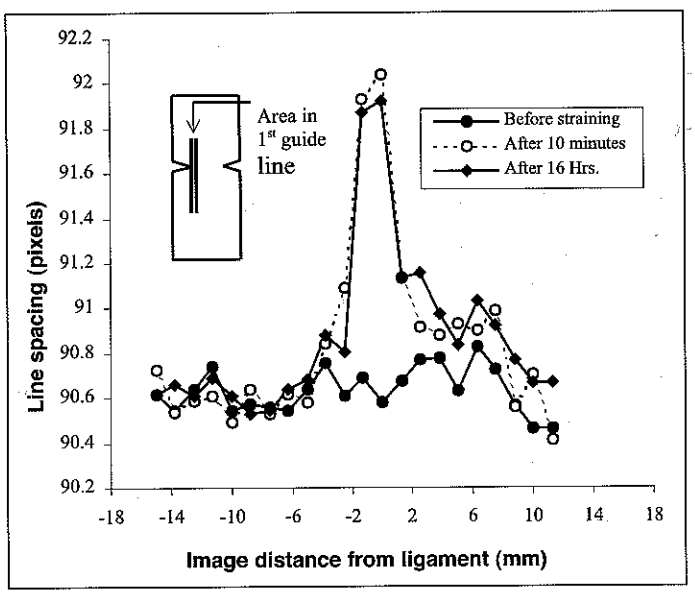

Fig. 9 Variation of line spacings with image distance (from the ligament, along 1st guide-line) for copy paper strained in the CD direction.

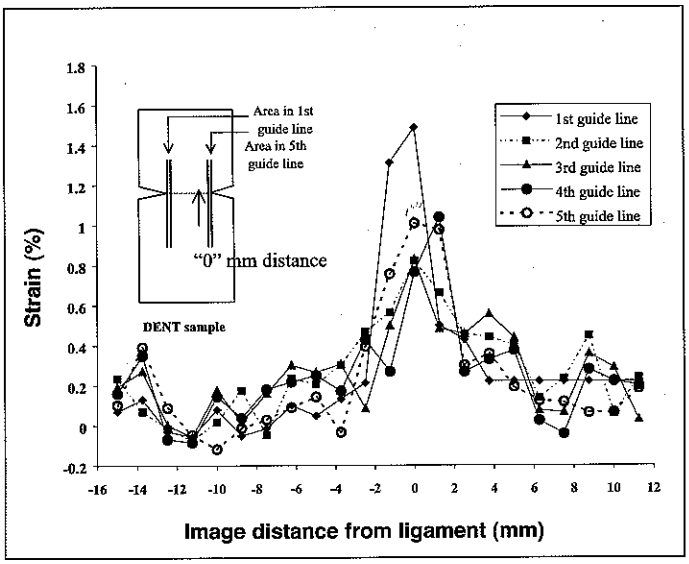

Fig. 10 Strain (%) versus image distance along each guide-line for copy paper in cross direction (CD) after straining. These data were taken after 16 hours conditioning.

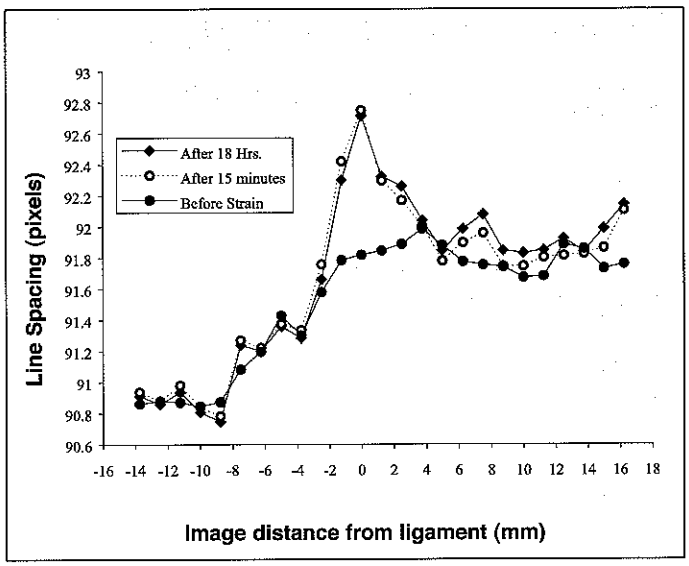

Fig. 11 Line spacing variation with image distance (from ligament), along 1st guide-line for MD direction.

4th guide-line was located 1.25 mm away from the ligament position. It is interesting to see that the irreversible strain field is getting broader (although less in magnitude) in the middle of the ligament compared to near the crack tip. The strain plots in Figure 10 indicate that the effective deformation field estimated along guide-lines 2 - 4 in the sample extended a distance of about 5 mm on both sides of the ligament. A significant variation of strain in the images taken from the same distance from the ligament but along different guide-lines, even well away from the notch-tips, is apparent. One reason for such behaviour could be due to variations in local strain fields, which is an obvious fact for a non-uniform material like paper. However, the appearance of negative strains suggests that there could be some differences in the image positions when capturing an image at a particular distance along one guide line, before and after straining.

The overall strain distributions along the guide-lines show that the deformation field is approximately elliptical or circular.

The line spacing in the MD, even before straining, showed considerable variation along the guide-lines (see Figure 11). This variation was more severe when paper was fed in the MD to the printer. The data shown below were obtained from a paper fed in the CD to reduce the variation. This must be the result of stresses applied by the printer. In the after-strain data, the highest magnitude of plastic strain occurs at the ligament.

The strain variation along the first three guide-lines from one of the crack tips is shown in Figure 12. It is quite significant that the plastic strain along the second and third guide-lines is almost negligible compared with that in the CD direction. This indicates that the deformation field is located only around the notches and does not extend over the whole ligament. However, the strain field for the CD sample has extended over the whole ligament of the sample.

According to Tanaka and Yamauchi's (*13*) classification, the development of the deformation pattern in the CD can be labelled as type II. Since L=15 mm and the deformation fields have extended to the whole ligament it is reasonable to label it as type II rather than type I. On the other hand, the deformation field in MD can be identified as type III, where the deformation field did not extend to form a single field.

CONCLUSIONS

This study shows that this new imaging technique can be used as a powerful tool to characterise the deformation fields in paper. This technique can be used to measure strains of less than 0.1% in this system. The plastic deformation field when straining in the CD was approximately elliptical or circular.

Continued page 482.

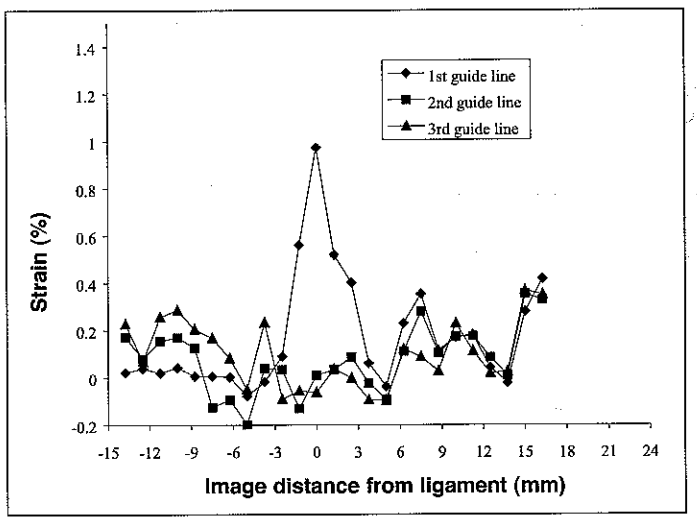

Fig. 12 Strain (%) versus image distance (from ligament) obtained along three guide-lines for copy paper in cross direction (MD) after straining. These data were taken after 18 hours conditioning.

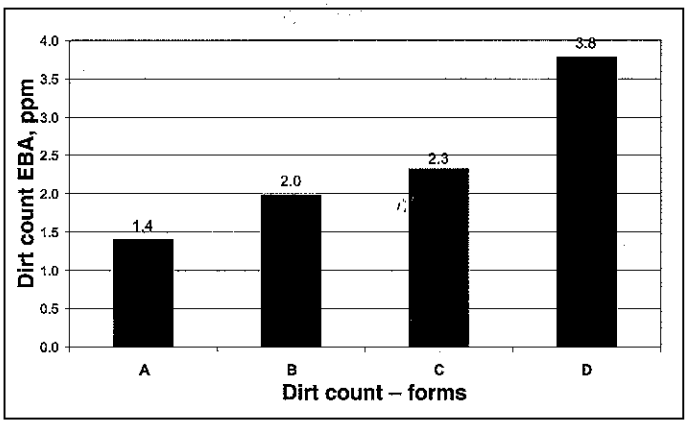

Fig. 13 Forms paper dirt count.

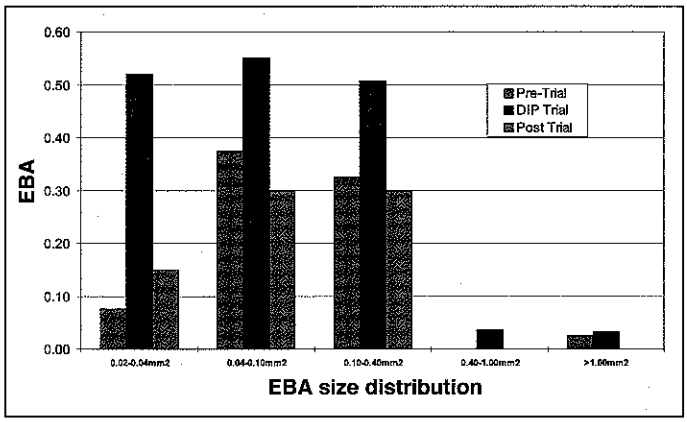

Fig. 14 Particle size distribution.

and indicate that there was a significant increase in the lower end of the particle size range (0.02 to 0.04 mm^2) compared with corresponding products made with no DIP.

CONCLUSIONS

A scanner-based system for measuring dirt has been developed at Amcor Research and Technology in conjunction with the Royal Melbourne Institute of Technology. Over a wide range of applications, the method has been found to be rapid and reliable, with good repeatability. Most importantly, it eliminates the inconsistency and observer bias associated with the visual measurement used in the past. The scanner system is also superior to camera-based systems in speed and area coverage and can be readily adapted to quality control measurement in a mill environment.

ACNOWLEDGEMENTS

The authors wish to acknowledge the assistance of Mike Pearce and his colleagues at the Fairfield Recycling Centre, for their technical and financial contribution to this study. The permission of Amcor Limited to publish the work is also gratefully acknowledged.

REFERENCES

(*1*) *TAPPI* Revised Method T563 pm-97 – Equivalent Black Area (EBA) and count of visible dirt in pulp, paper and paper board by image analysis, *TAPPI* Press (1997).

(*2*) Thurman, G. – Development of new TAPPI image analysis dirt count method and calibration standards, *Proc. TAPPI Process and Product Quality Conference*, Cincinnati, OH, USA, p.19 (1996).

(*3*) Jordan, B. D, Nguyen, N. G. and Bidmade, M. – Dirt counting with image analysis, *J. Pulp Pap. Sci.* **9**(2):TR60 (1983).

(*4*) *TAPPI* Test Method T213 om-89 – Dirt in pulp; and *TAPPI* Test Method T437 om-96 – Dirt in paper and paperboard, *TAPPI* Press.

(*5*) Jordan, B. D. and Nguyen, N. G. – Dirt counting with microcomputers, *J. Pulp Pap. Sci.* **11**(3):J73 (1985).

(*6*) Dyer, J. – New TAPPI method for dirt count using image analysis, *Prog. Pap. Recycling* **5**(3):20 (1996).

(*7*) Rosenberger, R. R. – Putting the new dirt count method into perspective – a discussion of TAPPI method T-563, *Prog. Pap. Recycling* **5**:9 (1996).

(*8*) Minutes of the meeting for the Image Analysis Dirt Method – TAPPI Joint Committee, Atlanta, GA (1998).

(*9*) Moss, C. S. – Issue-equality for all image analysis standardisation, *Proc TAPPI Process and Product Quality Conference*, TAPPI Press (1993).

(*10*) ISO FDIS 15755 – Estimation of contraries, Technical Committee CEN/TC 172; Pulp, Paper and Board. (Final Draft Dec. 1998).

Revised manuscript received for publication 7.1.00.

Continued from page 475.

ACKNOWLEDGEMENT

Financial support received from the CRC for Hardwood Fibre and Paper Science is gratefully acknowledged.

REFERENCES

(*1*) Roisum, D. R. – Runnability of paper Part 2: troubleshooting web breaks, *Tappi J.* **73**(2):101 (1990).

(*2*) Seth, R. S. and Page, D. H. – Fracture resistance: a failure criterion for paper, *Tappi* **58**(9):112 (1975).

(*3*) Westerlind, B. S., Carlsson, L. A. and Andersson, Y. M. – Fracture toughness of liner board evaluated by the J-integral, *J. Mat. Sci.* **26**:2630 (1991).

(*4*) Seth, R. S. and Page, D. H. – Fracture resistance of paper, *J. Mat. Sci.* **9**:1745 (1974).

(*5*) Mai, Y.-W. – Fracture resistance and fracture mechanisms of engineering materials, *Materials Forum* **11**:232 (1988).

(*6*) Rice, J. R. – A path independent integral and the approximate analysis of strain concentration by notches and cracks, *J. Appl. Mech.* **35**(6): 379 (1968).

(*7*) Cotterell, B. and Reddel, J. K. – The essential work of plane stress ductile fracture, *Int. J. Frac. Mech.* **13**(3):267 (1977).

(*8*) Fellers, C., Fredlund, M. and Wagberg, P. – Die-cutting toughness and cracking of corrugated board, *Tappi J.* **75**(4):103 (1992).

(*9*) Wellmar, P., Fellers, C., Nilsson, F. and Delhage, L. – Crack-tip characterization in paper, *J. Pulp Pap. Sci.* **23**(6):J269 (1997).

(*10*) Seth, R. S., Robertson, A. G., Mai, Y.–W. and Hoffman, J. D. – Plane stress fracture toughness of paper, *Tappi J.* **76**(2):109 (1993).

(*11*) Karenlampi, P. et al. – A comparison of two test methods for estimating the fracture energy of paper, *Tappi J.* **81**(3):154 (1998).

(*12*) Tanaka, A., Otsuka, Y. and Yamauchi, T. – In-plane fracture toughness testing of paper using thermography, *Tappi J.* **80**(5):222 (1997).

(*13*) Tanaka, A. and Yamauchi, T. – Size estimation of plastic deformation zone at the crack tip of paper under fracture toughness testing, *J. Pack. Sci. Technol.* **6**(5):268 (1997).

(*14*) Wiens, M. and Gottsching, L. – Determination of the critical J-integral for paper by means of image analysis, *Progress in Paper Physics-Seminar Proceedings*, p.135 (1996).

(*15*) Seth, R. S. – Measurement of in-plane fracture toughness of paper, *Tappi J.* **78**(10):177 (1995).

Revised manuscript received for publication 4.2.00.